Pure appl. geophys. 161 (2004) 1469–1487
0033 – 4553/04/071469 – 19
DOI 10.1007/s00024-004-2515-4



Pure and Applied Geophysics

# Intrusive Mechanisms at Mt. Etna Forerunning the July-August 2001 Eruption from Seismic and Ground Deformation Data

A. Bonaccorso[1], S. D'Amico[1], M. Mattia[1], and D. Patanè[1]

*Abstract* — In this work we present seismological and ground deformation evidence for the phase preparing the July 18 to August 9, 2001 flank eruption at Etna. The analysis performed, through data from the permanent seismic and ground deformation networks, highlighted a strong relationship between seismic strain release at depth and surface deformation. This joint analysis provided strong constraints on the magma rising mechanisms. We show that in the last ten years, after the 1991–1993 eruption, an overall accumulation of tension has affected the volcano. Then we investigate the months preceding the 2001 eruption. In particular, we analyse the strong seismic swarm on April 20–24, 2001, comprising more than 200 events ($M_{max}$ = 3.6) with prevalent dextral shear fault mechanisms in the western flank. The swarm showed a ca. NE-SW earthquake alignment which, in agreement with previous cases, can be interpreted as the response of the medium to an intrusive process along the approximately NNW-SSE volcano-genetic trend. These mechanisms, leading to the July 18 to August 9, 2001 flank eruption, are analogous to ones observed some months before the 1991–1993 flank eruption and, more recently, in January 1998 before the February-November 1999 summit eruption.

**Key words:** Ground deformation, volcano seismology, Mt. Etna Volcano, intrusive mechanism.

## *1. Introduction*

In the last twenty years, geophysical investigations have played an increasingly important role in studies of Mt. Etna eruptive processes. In particular, seismological and ground deformation studies provided the best information during recent years, in which several important lateral eruptions have occurred. It is well known that the study of seismic activity is a very powerful tool for understanding the inner structure of a volcano. Unfortunately, at Mt. Etna, the permanent seismic network has been of low density for a long time, limiting the accuracy of hypocentral locations, and consequently our expertise on Mt. Etna magma dynamics in the shallow 5 kilometres of crust (e.g., Gresta *et al.*, 1998; Barberi *et al.*, 2000; Patanè and Privitera, 2001). Only since the 90s have seismic data been available in digital form by a sufficient number of stations (increased in time) equipped also with three-component sensors (e.g., Patanè *et al.*, 1999; Patanè and Privitera, 2001; Patanè *et al.*,

[1] Istituto Nazionale di Geofisica e Vulcanologia – Sezione di Catania, Piazza Roma, 2, 95123 Catania, Italy. E-mail: bonaccorso@ct.ingv.it

2003a). This allows us to put high-quality constraints on seismic activity occurring at most depths and to better study the recent eruptive activity.

For the different recent lateral eruptions, ground deformation data analysis and modelling has indicated preparation times which lasted from months to several years. The modelling showed that the final uprising system, i.e., the tensile mechanisms inside the volcano edifice, involved the same structure oriented approximately NNW-SSE. A resumé of the ground deformation modelling of three principal recent lateral eruptions (1981, 1989, 1991–1993) and the implications in terms of associated precursors is discussed in BONACCORSO (2001). The NNW-SSE trending fault zone, older than Mt. Etna, borders on the eastern margin of Sicily crossing the volcano and characterises the main eruptive trend (e.g., FRAZZETTA and VILLARI, 1981; LO GIUDICE and RASÀ, 1986). The relationship of this regional trend with the regional tectonic setting, volcanological features and geophysical constraints is widely discussed in BONACCORSO *et al.* (1996).

In a wider and integrated context, a multidisciplinary investigation focussed on the eruption precursors should be implemented in order to better understand the possible modification of the volcanic activity. Recently, interesting results have been obtained through the integrated analysis of seismic and ground deformation data. Short-term precursors were observed by seismic foci migration with stress field modification (PATANÈ *et al.*, 1994; BONACCORSO *et al.*, 1996; Cocina et al., 1998) and transient variations on tilt during the two months preceding the 1991-1993 eruption (BONACCORSO and GAMBINO, 1997). Especially, the occurrence of strong seismic swarms, which occurred in the southwestern sector of the volcano along an approximately NE-SW structure, has been observed in relationship with magma movement through the upper crust and/or inside the volcanic edifice. This seismicity forerunning the 1991-1993 eruption has been interpreted as a response of the medium to the intrusive episode occurring across the volcano-genetic NNW-SSE structural trend (Fig. 1). Analogous conclusions have been reached for the swarm which occurred on January 1998 again in the southwestern flank (BONACCORSO and PATANÈ, 2001). Also in this case the seismic swarm was associated with an intrusion along the NNW-SSE trend which then led to the February-November 1999 summit eruption (Fig. 1).

In this work first we furnish wide evidence that after the 1991–1993 eruption, a tension accumulation characterised the volcano. Then we focus our study on investigating the final intrusive mechanisms which occurred during the period before the last lateral eruption occurring on July-August, 2001 (Research Staff of INGV-CT, 2001) as inferred by seismic strain release and surface 3-D deformation provided by the GPS permanent network. In particular, we analyse the strong seismic swarm of April 20–24, 2001. We show that this event is associated with the transition between a phase of continuous accumulation of tension below the volcano and the beginning of an intrusion process. Furthermore, we point out that this kind of seismicity can be, once again, considered a confirmation of the south western flank response to the intrusion processes occurring across the volcano-genetic, approximately NNW-SSE structural trend. We discuss the implications of this stress readjustment, which is to be considered a valid precursor.

## 2. Seismic and Ground Deformation Permanent Networks

The Mt. Etna permanent seismic network, run by the Catania Section of the National Institute of Geophysics and Volcanology (hereafter, INGV-CT), is the

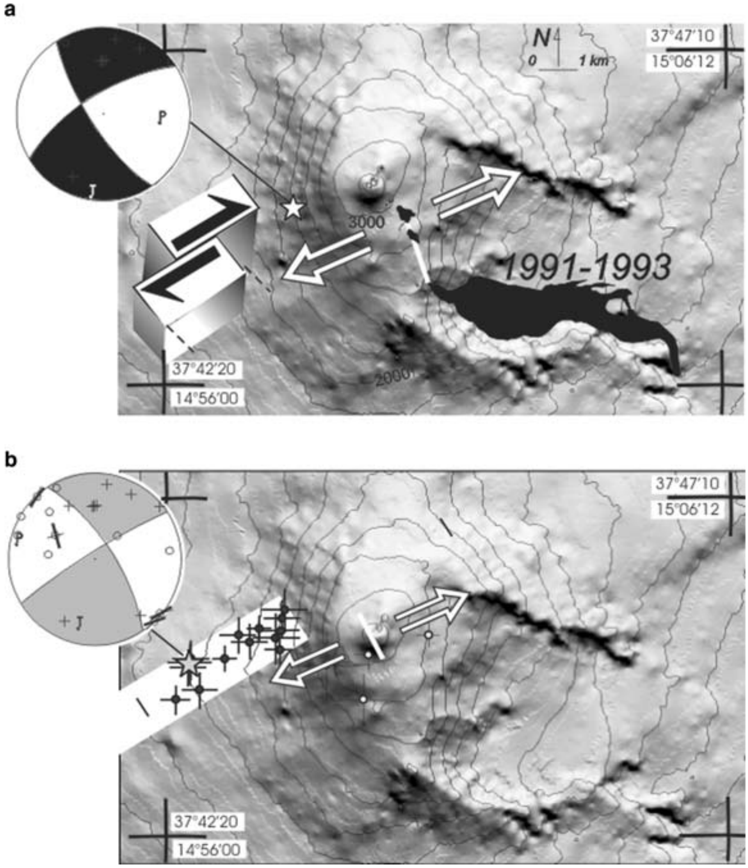


Figure 1
(a) Sketch model of the rupture mechanism associated with the 1991–1993 flank eruption (BONACCORSO *et al.*, 1996); (b) epicentral map of the January 9–14, 1998 seismic swarm. The position of the surface projection of the modelled shallow dike is also drawn (BONACCORSO and PATANÈ, 2001). The stars represent the main shocks of the swarms ($M_d = 4.5$ and $M_d = 3.7$, respectively). The focal solutions are also reported. The swarms were interpreted as shear response to the intrusion process along the NNW-SSE structural trend.

integration of two seismic networks running separately until 2000 by Istituto Internazionale di Vulcanologia (IIV) and Sistema Poseidon (Fig. 2). The former network was composed of 14 seismic stations, 10 of which were one-component analog stations, equipped with short-period sensors (1 s), and the other four three-component stations, two of which were equipped with broadband sensors (30 s). The Sistema Poseidon network was composed of 56 stations, spread out over eastern Sicily, 39 of which were deployed on Mt. Etna and equipped with short-period sensors (1 sec). Also in this case, excluding four three-component stations, the entire network was composed of one-component analog stations. Signals from remote sites are transmitted by radio or cable to Catania where they are continuously recorded on drum recorders and digitalized at a sampling rate varying from 100 Hz in continuous mode to 200 Hz in trigger mode.

The permanent network for the continuous tilt monitoring is composed of eight bi-axial electronic borehole tiltmeters positioned at about 3–5 m depth (Fig. 2). The complete configuration has been operating since 1990. The stations are equipped with Applied Geomechanics Inc. tiltmeters model 722 (CDV, MSC, MEG, SPC stations) with 0.1 $\mu$rad precision or model 510 (DAM, MDZ, MMT stations) with

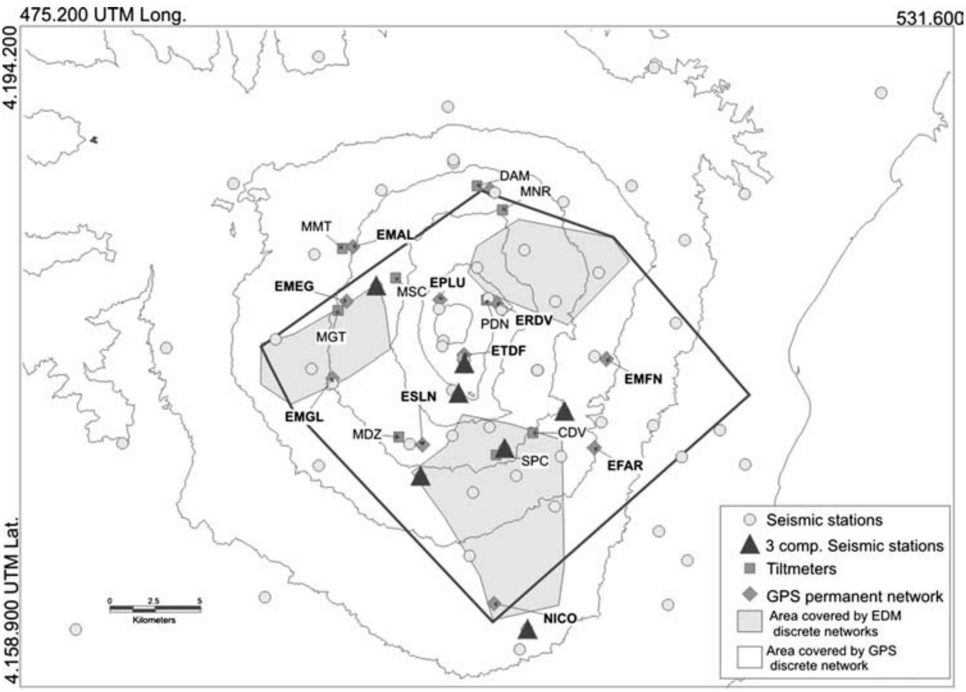


Figure 2
Mt. Etna seismic and ground deformation networks run by the Catania Section of the National Institute of Geophysics and Volcanology (INGV-CT).

0.01 $\mu$rad precision. The radial tilt, i.e., the component directed toward the crater, has positive signal variation that means crater up. The second component, the tangential one, is orthogonal to the radial and a positive signal variation means uplift in the anticlockwise direction. The control datalogger is programmed for 48 data/day sampling (1 sample every 30 minutes) and includes acquisition of the two tilt components, air and ground temperatures, and instrumental control parameters, such as power supply and dc/dc converter voltage. The data are transmitted to INGV-CT via radio-link. Temperature noise is present in the borehole types, whose electrolytic bubble sensors can be affected by diurnal and seasonal temperature variations (AGI, 1993; BONACCORSO *et al.*, 1999). The tilt data are filtered from the seasonal temperature noise using the linear correlation with the ground temperatures. In 1997 a high precision long-base fluid tiltmeter was installed at the Pizzi Deneri observatory (PDN.OBS) in the high (2850 m a.s.l.) northeastern volcano flank. The instrumentation is positioned along two underground tunnels, where two 80-m long orthogonal tubes are filled with mercury, whose vertical changes at the extremities are measured by laser sensors giving a real precision of 0.01 $\mu$rad (BONACCORSO *et al.*, 1998). It is stable and not affected by temperature noise because both the tilt measurement is obtained as the difference between vertical values of the mercury level at the extremities of the tubes and the sensors (optical laser) are very stable for temperature variations.

Recently the ground deformation continuous monitoring was upgraded with the installation of the GPS permanent network, which began to operate in November 2000. Only six stations were working until March 2001, while a configuration of 13 stations was reached in the late spring-summer of 2001 (Fig. 2). A PC-based master station, on which a software program (called Genesis Master) calls the remote stations (once or more per day), downloads GPS data through a Remote Access Server. Each remote station is based on an industrial PC motherboard and the transmission of data is performed by a GSM cellular modem. The gathered data are processed with software called EOLO (AMORE *et al.*, 2002), that one or more times per day processes the data and stores the processed baselines in a database. The same software displays data in terms of length variations between the benchmarks, and an automatic subroutine calculates the strain parameters and displays the areal dilatation, the shear components, the components of the strain tensor, etc. In off-line mode, a more accurate analysis can be performed with the Trimble Geomatics Office software. The network is adjusted using a same local reference point (NICO - Nicolosi), which can be considered fixed with respect to the summit area. Due to the small extension of the measured area, the tilt or bias introduced by differences in the satellite ephemeris reference systems are negligible. Therefore, the minimal constraint approach using one of the network benchmarks as a fixed point ensures the stability of the reference frame during different days. The error ellipse calculated at the confidence interval of 95% is of the order of a few millimeters. In Table 1 the main features of data processing are reported.

Table 1

*Method of GPS observations and analysis*

| | |
|---|---|
| Receiver | Trimble 4700 |
| Daily session | 6–24 h |
| Data sampling | 30 sec. |
| Elevation cutoff | 15° |
| Software | Trimble TGO |
| Orbit | precise eph. (NGS) |
| Tropospheric model | Saastamoinen's model with standard atmospheric conditions |
| Reference point | NICO (Nicolosi) |

### *3. Stress Accumulation after the 1991-1993 Lateral Eruption*

During the 1991-1993 eruption, the most significant lateral eruption in the last three centuries both in terms of duration (476 days) and lava erupted (ca. $250 \cdot 10^6$ $m^3$), the ground deformation showed a deflation of the volcano edifice, analysis of which constrained an intermediate storage at a depth of 3–4 km b.s.l. (BONACCORSO, 1996). A renewal of tension accumulation was observed in the whole volcanic edifice after the end of this eruption. The ground deformation showed an inflation (PUGLISI *et al.*, 2001) which uniformly increased during the following years. The areal deformation, accumulated by EDM and GPS networks from 1994 to 2001, indicated an overall continuous accumulation of tension inside the volcano (Fig. 3). It is noteworthy that this accumulation did not appear equilibrated by the energy discharge that occurred through the summit eruption (February-November, 1999), fed by a small dyke emplacement (BONACCORSO and PATANÈ, 2001), the January-May 2001 summit eruption, and the several tens of strong explosive events at the summit craters during the 1998–2001 (GVN, 1998; GVN, 2000; LA DELFA *et al.*, 2001; RESEARCH STAFF OF INGV-CT, 2001).

After the 1991-1993 deflation, the tilt signals evidenced a modest but progressive positive trend during the following years. The radial components, filtered from the seasonal thermic noise, are shown in Figure 4. The modest accumulation of tilt changes could be explained by a near uniform lifting of the volcano edifice. Also this pattern could be compatible with a tension accumulation inside the volcano. It is interesting to observe that in the last four years data of the summit long-base fluid tiltmeter has shown a near continuous deflation with about 14 microradians accumulated (Fig. 5) rather than inflation seen in the geodetic data. This interesting aspect could be an effect of the summit topography with average slope larger than 20° where a deep pressuring source can produce radial tilt opposite in sign to what would be expected for a flat topography (CAYOL and CORNET, 1998; WILLIAM and WADGE, 1998).

An overview of the seismicity occurring at Mt. Etna since 1990 is given by the rate of the earthquakes ($M_d \geq 2.5$) expressed as a number of events per day (inset in

Fig. 6). In Figure 6 the cumulative strain release is also reported. In detail, it is possible to observe that the 1991-1993 eruption was accompanied by a period of more or less total absence of earthquakes. The reappearance of such events was observed only since May 1993. The level of seismicity, however, was low until June 1996. Thereafter a significant increase in the seismic strain release gradient was observed and remained practically constant throughout 1997. In this last period seismicity affected most of the volcanic edifice (PATANÈ *et al.*, 1999) and was located at depths ranging from sea level to ca. 25 km. A strong increase in activity was recorded during the swarm occurring on January, 9–14, 1998 in the western flank of the volcano. Also this swarm was associated with an intrusive process

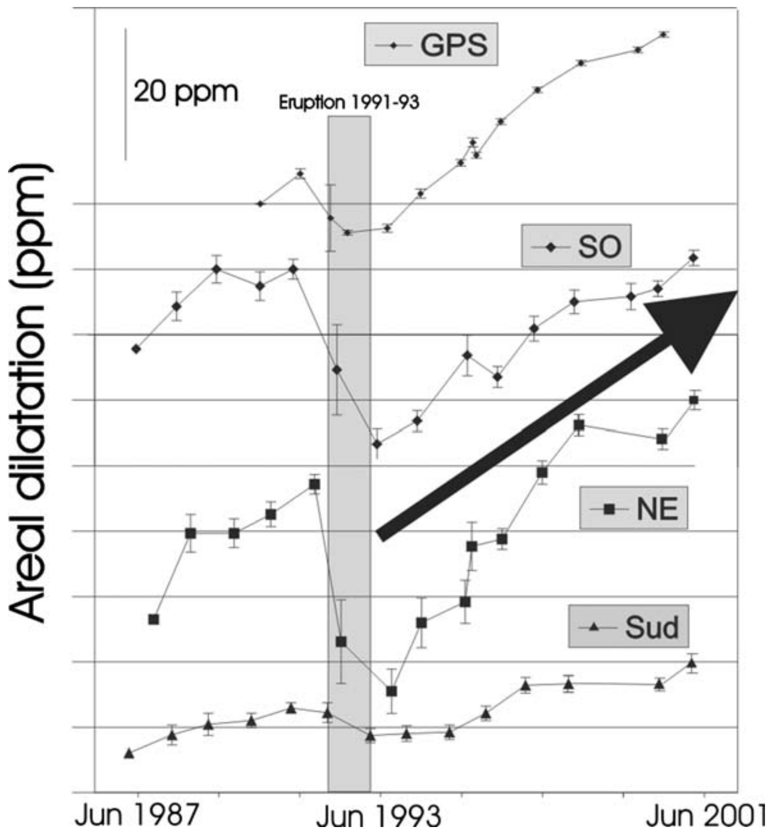


Figure 3
Planar areal dilatation calculated from the line length changes in the different monitored sectors through the EDM and GPS networks during the last 15 years. The areal dilatation represents mean values of the deformation in these areas. It is clearly evident how the 1991–1993 lateral eruption was accompanied by an areal contraction phase (deflation). After this eruption a near-continuous expansion accompanied the volcano edifice until 2001. A partial attenuation of the areal dilatation positive trend is recorded astride the February-November 1999 eruption.

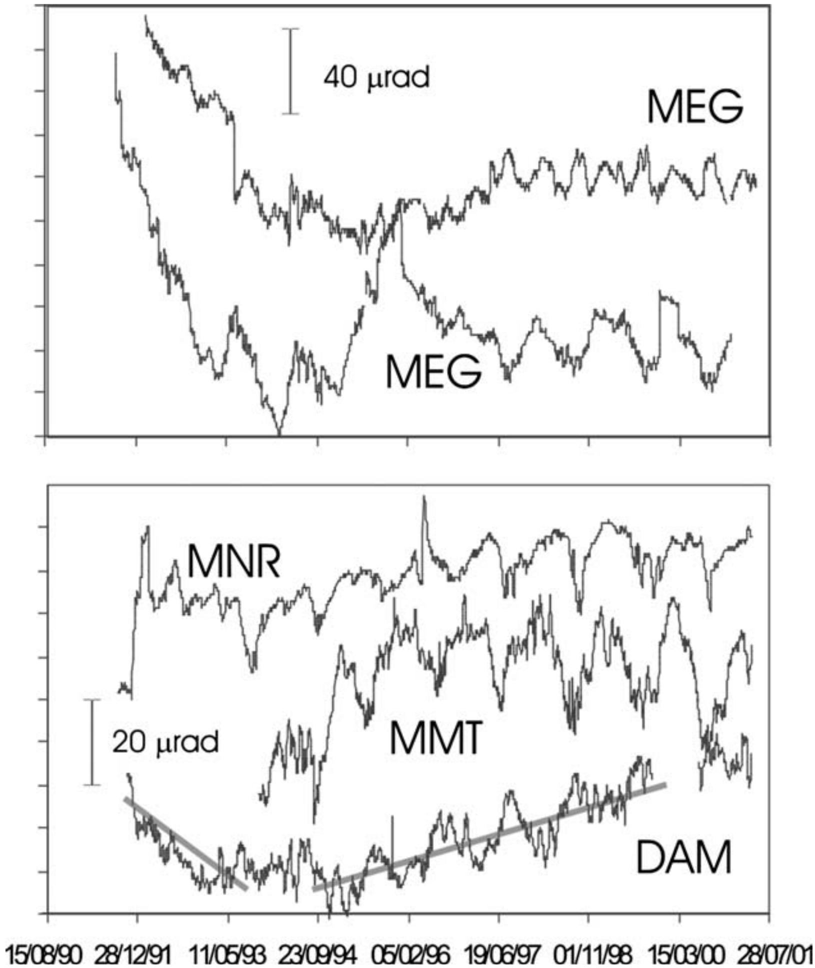


Figure 4

Radial tilt recorded at the shallow borehole stations during the period 1990–2001 before the July 2001 eruption onset. The data have been filtered from thermic seasonal noise using a linear correlation with the ground temperature. After the 1991–1993 deflation the signals evidence a modest but progressive inflation. The signals of the stations of MDZ, CDV, and SPC are not shown due to several interruptions which resulted from the electronic and instrumental problems which often caused the removing and re-installation of the instrumentation.

which provoked a shallow dike uprising inside the volcano edifice (BONACCORSO and PATANÈ, 2001). This dike was interpreted as the emplacement leading to the January-February 1999 eruption, which allowed a partial tension release. This interpretation is in agreement with the partial attenuation of the areal dilatation trend (see Fig. 3) and the low seismic level mainly recorded in the second half of 1999.

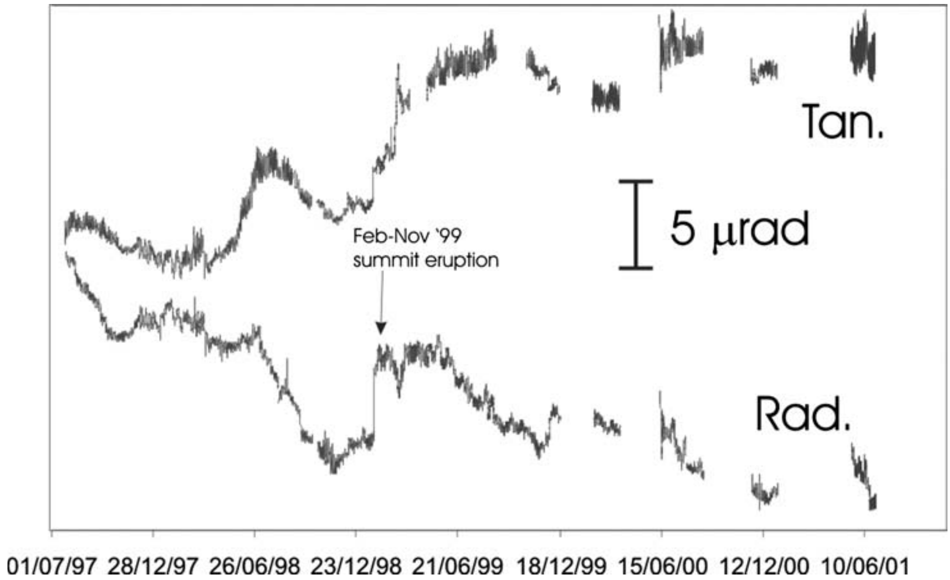


Figure 5
Radial tilt recorded at the long-base mercury tiltmeter during 1997–2001 before the July 2001 eruption onset (raw data). The station is located in the northeastern summit area (2850 m a.s.l.).

After several months of low seismic activity, a significant variation in the strain release gradient was observed from November 5, 2000, when a seismic swarm occurred in the upper southern flank of the volcano (115 earthquakes; $M_{max} = 3.6$) at a depth of ca. 8–10 km. This swarm marked the beginning of a relevant positive variation in the cumulative strain release curve (Fig. 6). In the following months other relevant swarms occurred and the average number of "background" events also increased together with the mean magnitude.

### *4. January – April 2001 Seismicity and Ground Deformation*

Focusing our attention now on the spatial distribution of seismicity during the period 1 January–19 April 2001, in Figure 7 the map of epicentral locations and the related west-east cross section are reported. Earthquakes were located using HYPOELLIPSE code (LAHR, 1989) so as to allow for the difference in altitude of the seismic stations and to correctly detect the hypocentre spatial patterns in the volcanic cone. The 1-D velocity model used was derived by HIRN *et al.* (1991), with sea level assumed as the reference (zero) elevation. We selected 232 events using the following thresholds: number of observations (N) $\geq$ 10, the horizontal 68% confidence limit in the least well-constrained direction (ERH) $\leq$ 1.0 km, the 68% confidence limit for depth (ERZ) $\leq$ 1.5 km, root-mean-square residual (RMS) $\leq$ 0.3 s,

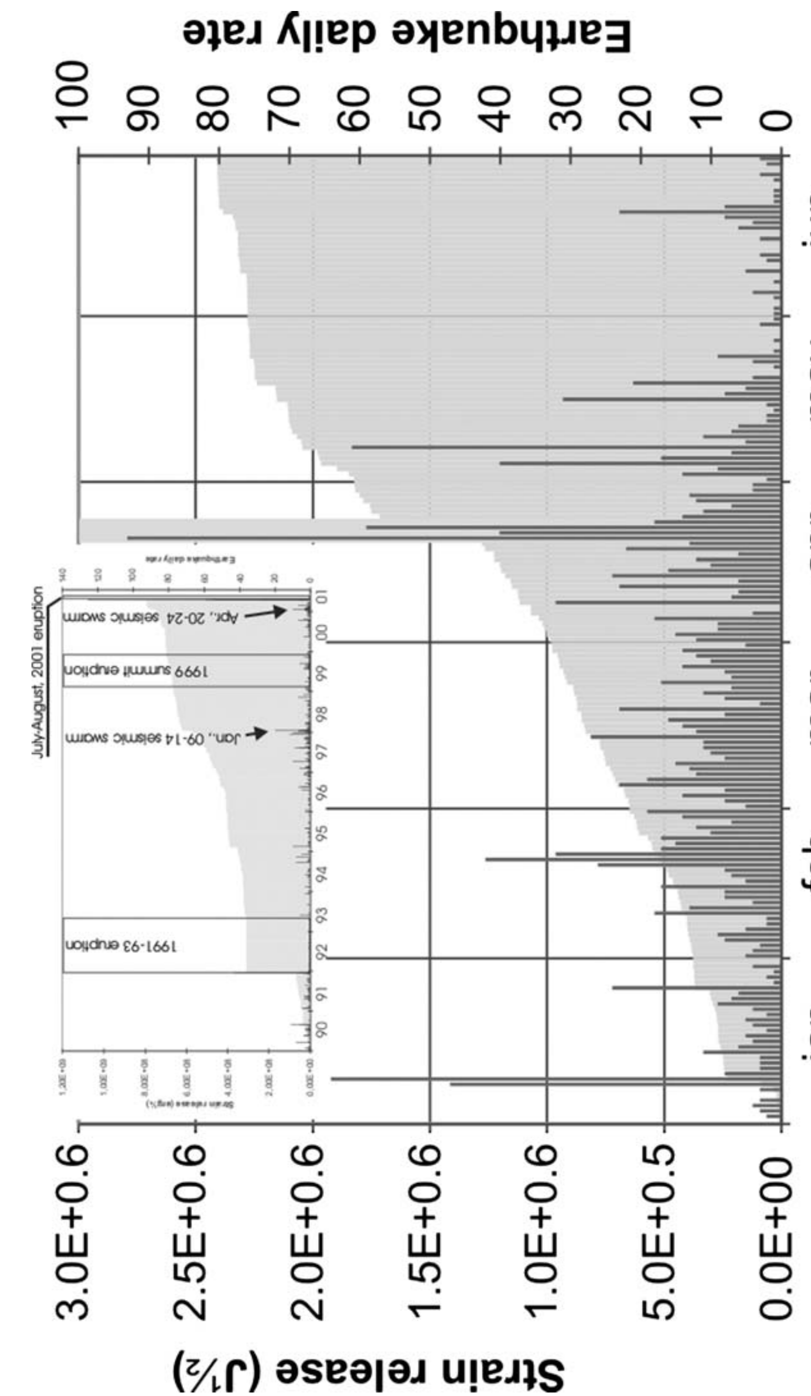


Figure 6

Number of earthquakes ($M_d \geq 1.0$) and related strain release vs. time recorded in the Etnean area during January-July 2001 time period. In the inset, the number of earthquakes ($M_d \geq 2.5$) and related strain release vs. time recorded during 1990-July 2001 is also shown.

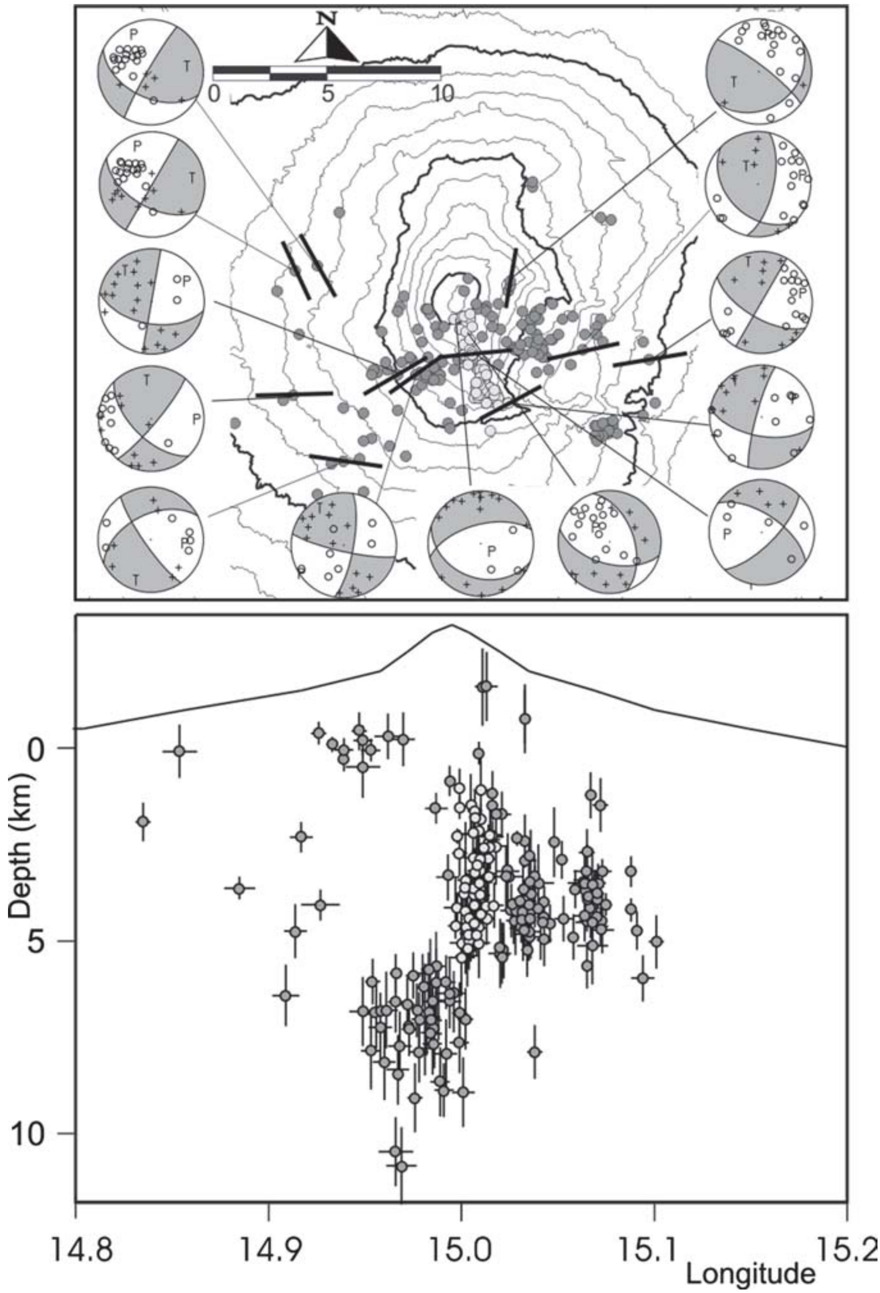


Figure 7
Map of epicentral locations and related W-E cross section of the best constrained earthquakes recorded between January and 19, April, 2001. FPSs of some stronger earthquakes and the related azimuth distribution of the horizontal projection of $P$ axes are also shown.

largest azimuthal separation in degrees between stations as seen from the epicenter (GAP) $\leq 180°$. Earthquake epicenters spread in a wide area covering most of the southern and eastern part of the volcano (Fig. 7). A peculiar feature of the earthquakes spatial distribution is its depth pattern. In fact, in the W-E cross section we can observe that the seismicity of the eastern flank is confined to the depth range 2–6 km b.s.l., while, in the central-western flank shocks are confined in two main different volumes, under ca. 6 km and above 1 km b.s.l., respectively. Moreover, since the second half of February, an increase in the seismicity has also been observed in the central upper part of the volcano. Earthquake locations show a ca. NNW-SSE alignment, and focal depths range between 1 and 5 km b.s.l. (light grey circles in Fig. 7). In Figure 7 thirteen Fault Plane Solutions (FPS) of the stronger earthquakes which occurred in this period and the related spatial *P*-axes distribution are also reported. These FPSs have been selected on the basis of rigorous criteria (number of polarities $\geq 15$, number of polarity discrepancies $\leq 2$, focal planes uncertainty $< 20°$, unique and unambiguous solution). FPSs show prevalent strike-slip rupture mechanisms and, in several cases, these strike-slip faults present a remarkable normal component. Normal dip-slip mechanisms were also observed along the alignment oriented NNW-SSE where seismicity was mainly clustered. Southwards of the central craters the *P*-axes orientation indicate a ca. E-W direction, coherently with the ground deformation results which indicated a similar orientation of the displacement vectors for this sector of the volcano. Conversely, at greater depth ($> 15$ km) earthquakes located in the western and northwestern sector of the volcano displays a different orientation of *P*- and *T*- axis with respect to the shallower ones. In fact, we usually observe that *P*-axes are ca. NNW-trending below 15-km depth, suggesting a closer relation with the regional stress at greater depth (PATANÈ and PRIVITERA, 2001; PATANÈ *et al.*, 2003). It is noteworthy, excepting the deep earthquakes recorded in the southwestern sector (Jan.-April, 2001), that this seismicity shows similar features to that observed during the July, 12–18 seismic swarm, which led to the lateral eruption of July 17 to August 9 (RESEARCH STAFF OF INGV-CT, 2001), with prevalent dip-slip rupture mechanism (PATANÈ *et al.*, 2003a). The main difference is that before the eruption the foci were located at shallow depth.

A powerful contribution to continuous ground deformation monitoring was provided by the GPS permanent network. Coherently with the renewal of seismic activity observed since November 2000, during the early months of 2001 the daily length variations between the stations of the GPS permanent network followed the general trend measured once per year since the end of the 1991-1993 eruption, and confirmed that the inflation of the volcano continued (Fig. 8). Moreover, the height changes showed a clear positive trend during the period between January and the $20^{th}$ of April 2001 in agreement with the continuation of the inflation phase. The distribution of the displacement vectors together with the vertical changes calculated for the period January 12 to April 20 is shown in Figure 9.

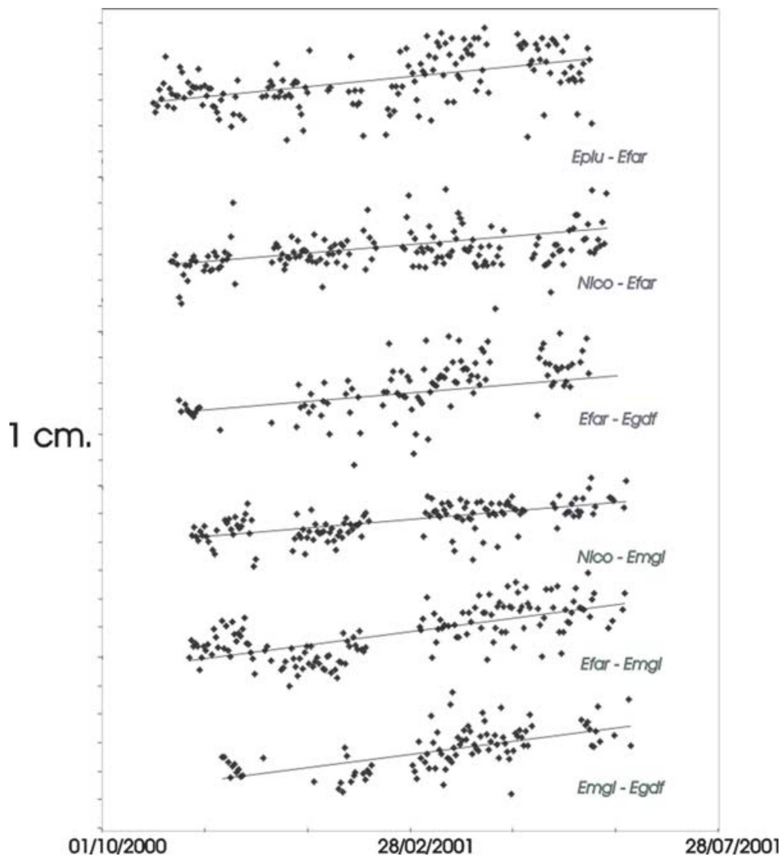


Figure 8
Example of line length changes observed by the daily sessions of the GPS permanent network during January-June 2001. Continuing the previous eight-year trend, a near continuous expansion is still evident. This expansion was to be interrupted by the July 2001 eruption.

## *5. The Swarm of April 20-24, 2001*

On April 20, 2001 a strong seismic swarm started and more than 200 events ($M_{max} = 3.6$) were recorded in about four days. We selected 41 events using the following thresholds: number of observations ≥ 10, ERH ≤ 1.0 km, ERZ ≤ 1.0 km, RMS ≤ 0.30 s, GAP ≤ 180°. The epicenters distributed in the southwestern upper part of the edifice clearly define a NE-SW alignment located between ca. 5 and 10 km depth (Fig. 10). The epicentral distribution is in agreement with the rupture mechanism obtained by the focal plane solution of the main shock (star in Fig. 10) and then constrains the fault plane to be along a NE-SW direction. In Figure 8 we report the FPSs of ten shocks selected on the basis of rigorous criteria (number of polarities ≥ 15, number of polarity discrepancies ≤ 2, focal planes uncertainty < 20°,

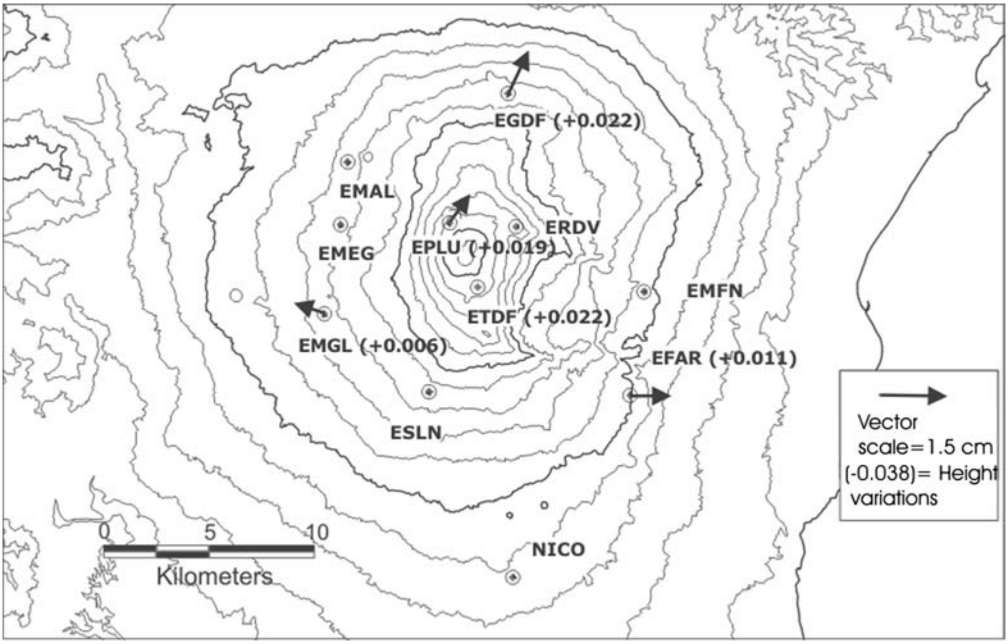


Figure 9
Displacement vectors and vertical changes (ellipsoidal) calculated for the time interval January 01, 2001 to April 26, 2001 The reference point is NICO. The error ellipse calculated at the confidence interval of 95% is of the order of a few millimetres.

unique and unambiguous solution). The analysis was performed using the FPFIT algorithm (REASENBERG and OPPENHEIMER, 1985) to plot first motion data and to evaluate nodal planes and the orientation of main strain axes. The good azimuth coverage of the investigated area well constrained the single focal solutions for most of the events. Coherently with the rupture mechanism of the main shock (star in Fig. 10), which is of dextral strike-slip, the majority of the other earthquakes present comparable rupture mechanisms. In Figure 10 the spatial distribution of the horizontal projection of the *P*-axes for these mechanisms is also reported. *P*-axes directions are mostly distributed almost horizontally, showing a prevalence of compression in the N90°–110°E direction.

Important information pertaining to the deformative behaviour of the volcano during the seismic crisis is provided by the GPS permanent network. The positive areal dilatation pattern, which was evidenced by EDM and GPS discrete networks since 1994 and was also confirmed during the early months by daily GPS measurements, appears interrupted during the week of the swarm (Fig. 9). The main aspect is represented by the negative vertical changes which indicate a lowering at the entire volcano scale (Fig. 11). This behaviour is compatible with magma movements from depth into the shallow (3–5 km) reservoir (PATANÈ *et al.*,

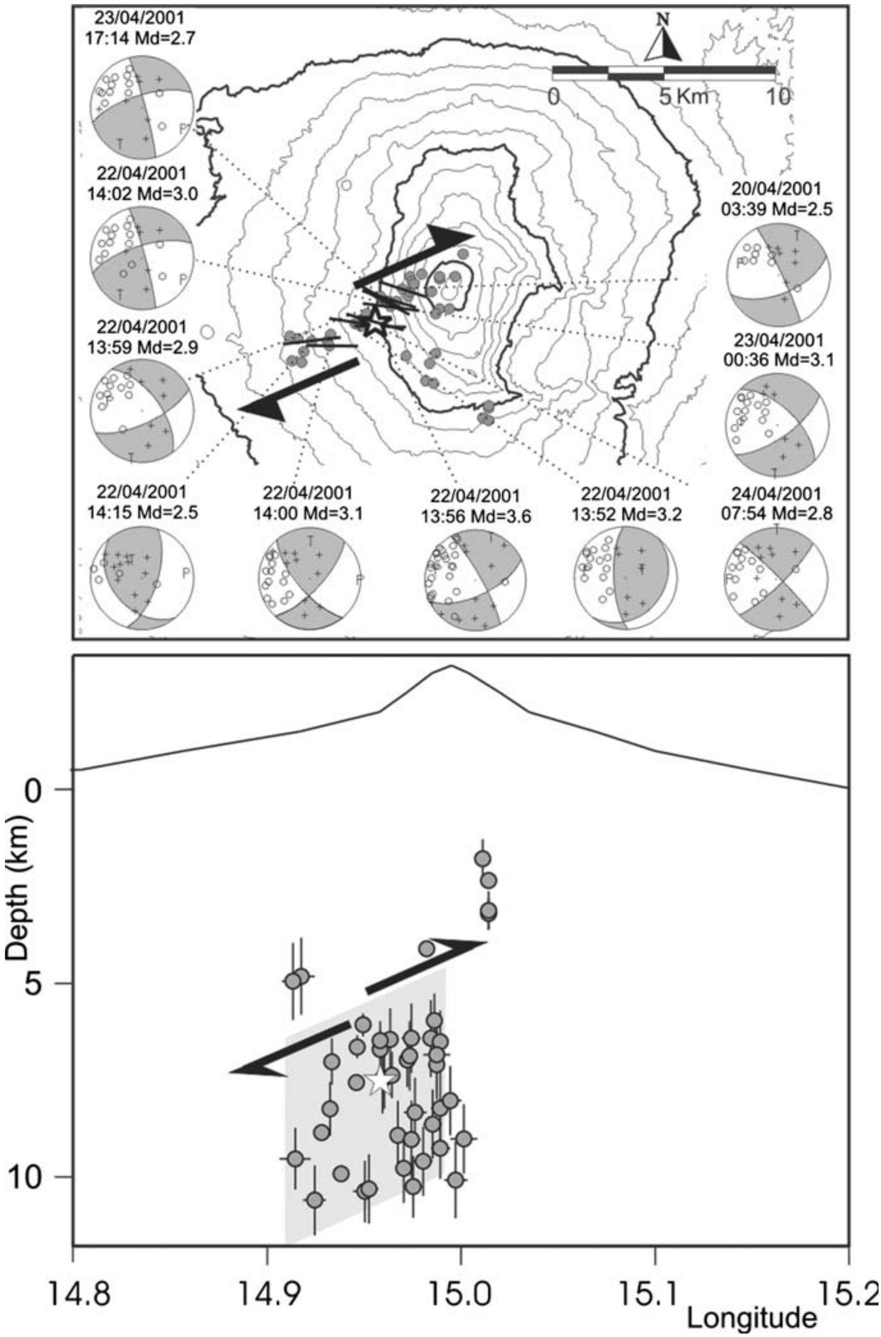


Figure 10
Epicentral map and hypocentral W-E cross section of the best constrained earthquakes of the swarm recorded between, April 20–24, 2001. Some examples of FPSs and the related azimuth distribution of the horizontal projection of *P* axes are also reported.

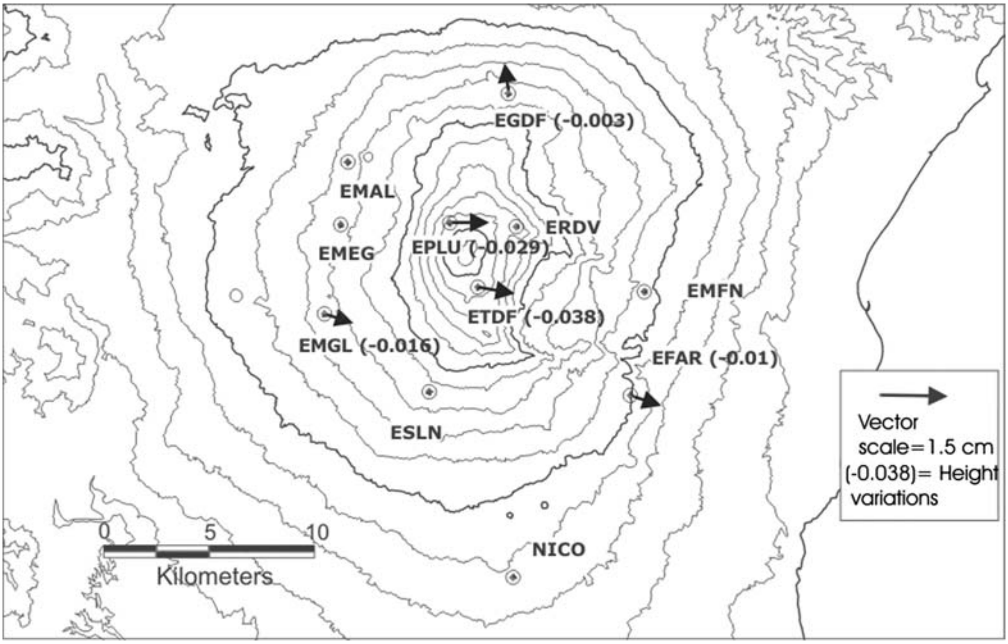


Figure 11
Displacement vectors and vertical changes calculated for the time interval 20–26 April, astride the seismic swarm. The reference point is NICO. The error ellipse calculated at the confidence interval of 95%. is of the order of a few millimetres.

2003b) which causes a temporary decrease of the pressure at depth and the edifice deflation.

## 6. *Concluding Remarks*

In this work we present an overview of seismic activity and ground deformation observed at Mt. Etna in recent years, focusing our attention on the last few months before the July-August 2001 eruption. After the 1991–1993 eruption, the areal dilatation highlights that the volcano is recharged with a near continuous constant rate, whereas during the same period the seismicity mainly exhibits two different behaviours: it is practically negligible (except during some swarms which occurred from late 1994 until early 1995) until June 1996 and then gradually increases from July 1996 until the beginning of 1999, when a ten-month summit eruption took place. During this time interval (1996–1999) the spread and deep seismicity and the overall and marked inflation of the entire edifice suggest that the pressure centre could be several kilometres deep (5–10) below the sea level. In this period the tension accumulation was partially released through an intense summit activity (lava fountains, overflows from central craters, and summit eruptions). Thereafter, the seismicity remained at low levels until November 2000, when a strong seismic swarm marked a new significant modification in the seismic strain release. In the ensuing months the average number of "background" events increased together with the mean magnitude, and several swarms also occurred. A marked change in the state of the volcano was represented by the April 20–24, 2001 seismic swarm, which occurred in the southwestern flank. Following this swarm, a further increase in the strain release gradient was observed until May 20, slightly before the beginning of a cycle of Strombolian eruptions at the southeast Crater. This strong seismic swarm represents the response of the medium to a deep magma intrusive episode that started in the preceding months and uprose at a shallower depth in the following months, and was a forerunner of the July 17 to August 10, 2001 lateral eruption (RESEARCH STAFF OF INGV-CT, 2001). This intrusion seems to be testified by the seismicity clustered along the NNW-SSE direction, which occurred in the period January-April, 2001 and by a clear pattern evidenced by geodetic data. Particularly, the polarization of the displacement vectors in the east direction can be considered as the result of magma intrusion along the same structures activated seismically.

Gravity measurements before the 2001 eruption show a progressive negative variation which reversed its trend between July 2001 and the beginning of August 2001 when the eruption occurred. This has been interpreted as the effect of a 2–3 * $10^{11}$ kg mass decrease within a source 2–3 km b.s.l. that could have supplied the 2001 eruption (RESEARCH STAFF OF INGV-CT, 2001). However, in our opinion, the interpretation of gravity changes alone may not be sufficient to describe an intrusion or magma recharge processes (FERNÁNDEZ *et al.*, 2001a,b). In fact, gravity measurements on Mt. Etna are performed periodically along a profile of 19 stations crossing east-west the uppermost southern flank of the volcano and no continuous recording was still available.

From the integration of seismological and geodetic data, in this work we have evidence that before the July-August 2001 eruption an intrusive mechanism took place along the volcano-genetic NNW-SSE structural trend, where dike emplacement caused several recent eruptions (e.g., BONACCORSO, 2001). In particular, similar mechanisms were observed before the 1991–1993 eruption (e.g., BONACCORSO *et al.*, 1996) and in January 1998 (BONACCORSO and PATANÈ, 2001). As regards the April 2001 swarm, an interesting contribution is provided by the new GPS permanent network which during the period of the swarm (20–24 April) showed a general lowering of the volcano edifice. This behaviour could be explained by the intrusion process which is characterised by a mass transfer from a deeper storage zone (5–10 km b.s.l.) to the upper part of the volcano.

The uprising of melt from the overpressured reservoir causes a depressuring of the same reservoir. The lowering of the edifice recorded during the magma ascent and the associated swarm would be the consequent deformation effect recorded on the surface. This interesting aspect would confirm the possible existence of magma storages inside Mt. Etna and provide the basis for future investigations.

In conclusion, the integration of seimicity, i.e., the fast strain release along preferential structures, together with the ground deformation, i.e., slow movement of the overall edifice, proves to be a powerful tool to further knowledge of the volcano and to understand its dynamics.

## *Acknowledgments*

We acknowledge the helpful comments and suggestions of P. Davis and J Fernandez regarding the manuscript. This work was supported by grants from the Gruppo Nazionale per la Vulcanologia of INGV.

## References

Amore, M., Bonaccorso, A., Ferrari, F., and Mattia, M. (2002), *EOLO: Software for the Automatic On-line Treatment and Analysis of GPS Data for Environmental Monitoring*, Computer and Geosciences *28*, *2*, 271–280

Applied Geomechanics Incorporated (1993), *Notes on Temperature Coefficients and Long-term Drift of Applied Geomechanics Tiltmeters*, Report no. A-93-1001, AGI, Santa Cruz, California.

Barberi, G., Cocina, O., Neri, G., Privitera, E., and Spampinato, S. (2000), *Volcanological Inferences From Seismic Strain Tensor Computation at Mt. Etna Volcano, Sicily*, Bull. Volcanol. *62*, 318–330.

Bonaccorso, A., Falzone, G., Raia, G., and Villari, L. (1998), *Application for New Technology for Ground Deformation Continuous Detection*, Acta Vulcanol. *10 (1)*, 7–12.

Bonaccorso, A., Falzone, G., and Gambino S. (1999), *An Investigation into Shallow Borehole Tiltmeters*, Geophys. Res. Lett. *26*, 1637–1640.

Bonaccorso, A., Ferrucci, F., Patanè, D., and Villari, L. (1996), *Fast Deformation Processes and Eruptive Activity at Mt. Etna (Italy)*, J. Geophys. Res. *101*, 17,467—17,480.

Bonaccorso, A. (1996), *A Dynamic Inversion for Modelling Volcanic Sources through Ground Deformation Data (Etna 1991–1992)*, Geophys. Res. Lett. *23*, 451–454.

Bonaccorso, A. and Gambino, S. (1997), *Impulsive Tilt Variations at Mount Etna Volcano (1990–1993)*, Tectonophysics *270*, 115–125

Bonaccorso, A. (2001*), Mt Etna Volcano: Modelling of Ground Deformation Patterns of Recent Eruptions and Considerations on the Associated Precursors*, J. Volcanol. Geotherm. Res. *109*, 99–108.

Bonaccorso, A. and Patanè, D. (2001), *Shear Response to an Intrusive Episode at Mt. Etna Volcano (January 1998) Inferred through Seismic and Tilt Data*, Tectonophysics, *334*, 61–75.

Cayol, V. and Cornet F. H. (1998), *Effects of Topography on the Interpretation of the Deformation Field of Prominent Volcanoes – Application to Etna*, Geophys. Res. Lett. *23*, 1979–1982.

Cocina, O., Neri, G., Privitera, E., and Spampinato, S. (1998), *Seismogenic Stress Filed beneath Mt. Etna (South Italy) and Possible Relationships with Volcano-tectonic Features*, J. Volcanol. Geotherm. Res. *83*, 335–348.

Fernández, J., Charco, M., Tiampo, K. F., Jentzsch, G., and Rundle, J. B. (2001a), *Joint Interpretation of Displacement and Gravity in Volcanic Areas. A Test Example: Long Valley Caldera, California*, Geophys. Res. Lett. *28*, 1063–1066.

Fernández, J., Tiampo, K. F., Jentzsch, G, Charco, M., and Rundle, J. B. (2001b), *Inflation or Deflation?: New Results for Mayon Volcano Applying Elastic-gravitational Modeling*, Geophys. Res. Lett. *28*, 2349–2352.

Frazzetta, G. and Villari, L. (1981), *The Feeding of the Eruptive Activity of Etna Volcano: The Regional Stress Field as a Constraint to Magma Uprising and Eruption*, Bull. Volcanol. *44*, 269–282.

Gresta, S., Peruzza, L., Slejko, D., and Di Stefano, G. (1998), *Inferences on the Main Volcano-tectonic Structures at Mt. Etna (Sicily) from a Probabilistic Seismological Approach*, J. Seismol. *2*, 105–116.

GVN (1998), *Global Volcanism Network, Bulletin of the Global Volcanism Program of the Smithsonian Institution*, Washington DC, vol. 23.

GVN (2000), *Global Volcanism Network, Bulletin of the Global Volcanism Program of the Smithsonian Institution*, Washington DC, vol. 3.

Hirn, A., Nercessian, A., Sapin, M., Ferrucci, F., and Wittlinger, G. (1991), *Seismic Heterogeneity of Mt. Etna: Structure and Activity*, Geophys. J. Int. *105*, 139–153.

La Delfa, S., Patanè, G., Clocchiatti, R., Joron, J. L., and Tanguy, J. C. (2001), *Activity Preceding the February 1999 Fissure Eruption: Inferred Mechanism from Seismological and Geochemical data*, J. Volcanol. Geoth. Res. *105*, 121–139.

Lahr, J. C. (1989), *HYPOELLIPSE/VERSION 2.0* : A Computer Program for Determining Local Earthquake Hypocentral Parameters, Magnitude, and First-motion Pattern*, U. S. Geol. Survey, Open-File Report 89/116, 81 pp.

Lo Giudice, E. and Rasà, R. (1986), *The Role of the NNW Structural Trend in the Recent Geodynamic Evolution of Northeastern Sicily and its Volcanic Implications in the Etnean Area*, J. Geodyn. *5*, 309–330.

Patanè, D., Privitera, E., Ferrucci, F., and Gresta, S. (1994), *Seismic Activity Leading to the 1991–93 Eruption of Mt. Etna and its Tectonic Implications*, Acta Vulcanol. *4*, 47–56.

Patanè, D., Ferrari, F., and Ferrucci, F. (1999), *First Application of ASDP Software: A Case Study at Mt. Etna Volcano and in the Acri Region (Southern Italy)*, Phys. Earth Planet. Inter. *113*, 75–88.

Patanè, D. and Privitera, E. (2001), *Seismicity Related to 1989 and 1991–93 Mt. Etna (Italy) Eruptions: Kinematic Constraints by FPS Analysis*, J. Volcanol. Geotherm. Res. *109*, 77–98.

Patanè, D., Privitera, E., Gresta, S., Alparone, S., Akinci, A., Barberi, G., Chiaraluce, L., Cocina, O., D'Amico, S., De Gori, P., Di Grazia, G., Falsaperla, S., Ferrari, F., Gambino, S., Giampiccolo, E., Langer, H., Maiolino, V., Moretti, M., Mostaccio, A., Musumeci, C., Piccinini, D., Reitano, D., Scarfì, L., Spampinato, S., Ursino, A., and Zuccarello, L. (2003a), *Seismological Features and Kinematic Constrains for the July-August 2001 Lateral Eruption at Mt. Etna Volcano, Italy,* Annali di Geofisica, in press.

Patanè, D., De Gori, P., Chiarabba, C., and Bonaccorso, A. (2003b), *Magma Ascent and the Pressurization of Mount Etna's Volcanic System*, Science, *299*, 2061–2063.

Puglisi, G., Bonforte, A., and Maugeri, S. R. (2001), *Ground Deformation Patterns on Mt. Etna, between 1992 and 1994, Inferred from GPS Data*, Bull. Volcanol. *62*, 371–384.

Reasenberg, P. and Oppenheimer, D. (1985), FPFIT, FPPLOT, and FPPAGE: FORTRAN Computer Programs for Calculating and Displaying Fault Plane Solutions, U.S. Geol. Surv. Open File Rep. *85/739*, 109 pp.

Research Staff of INGV-CT (2001), *Multidisciplinary Approach yields Insight into Mt. Etna Eruption*, EOS Trans. Am. Geophys. Uni. *82*, 653–656.

Williams, C. A. and Wadge, G. (1998), *The Effects of Topography on Magma Chamber Deformation Models: Application to Mt. Etna and Radar Interferometry*, Geophys. Res. Lett. *25*, 1549–1552.

(Received February 11, 2002, revised February 28, 2003, accepted March 14, 2003)